

Anisotropy and domain formation in a dipolar magnetic metamaterial

Einar Digernes,¹ Anders Strømberg,¹ Carlos A. F. Vaz,² Armin Kleibert,² Jostein K. Grepstad,¹ and Erik Folven^{1, a)}

¹⁾Norwegian University of Science and Technology, Department of Electronic Systems, 7491 Trondheim, Norway

²⁾Swiss Light Source, Paul Scherrer Institut, 5232 Villigen PSI, Switzerland

(Dated: 1 July 2021)

Long-range magnetic ordering can be stabilized in arrays of single-domain nanomagnets through dipolar interactions. In these metamaterials, the magnetic properties are determined by geometric parameters such as the nanomagnet shape and lattice symmetry. Here, we demonstrate engineering of the anisotropy in a dipolar magnetic metamaterial by tuning of the lattice parameters. Furthermore, we show how a modified Kittel's law explains the resulting domain configurations of the dipolar ferromagnetic arrays.

In magnetic metamaterials made from arrays of single-domain nanomagnets,^{1,2} long-range magnetic order can emerge as a result of dipolar interactions.³⁻⁷ The nature of this ordering is determined by the nanomagnet shape and the lattice symmetry of the array.

The stray field of a single-domain nanomagnet can be approximated to that of a dipole. For circular disks, the magnetization will have in-plane shape anisotropy. As pointed out by Politi et al.,⁸ it is helpful to think of an array of nanomagnets as composed of chains of magnetic dipoles, where the dipole interaction results in ferromagnetic alignment of the spins along the length of each chain. The coupling between neighboring chains favors ferromagnetic or antiferromagnetic ordering dependent on the lattice symmetry, and the coupling between chains decreases exponentially with increasing separation.⁸⁻¹⁰

Long-range ordering of magnetic point dipoles on a crystalline lattice was first described by Luttinger and Tisza^{11,12} and later by Rozenbaum¹³ for two-dimensional arrays. Ferromagnetic order was predicted for a hexagonal lattice and antiferromagnetic order for a square lattice. This magnetic order is reinforced when taking into account the finite size of the disks.¹⁴

Experimental exploration of dipolar magnetic metamaterials is scarce, presumably due to the challenges of fabricating nanomagnet arrays with a low blocking temperature and strong dipole-dipole interactions. State-of-the-art electron beam lithography now facilitates fabrication of such metamaterials in which the geometric parameters are controlled with a precision of a few nanometers.^{4-7,15}

In this work, the domain formation in dipolar magnetic metamaterials with antiferromagnetic and ferromagnetic ordering is controlled by changing the spacing of the nanomagnets. The magnetic domain structure was imaged using x-ray magnetic circular dichroism photoemission electron microscopy (XMCD-PEEM). Our work demonstrates how the unit cell symmetry and size provide handles for tuning the magnetic properties of these metamaterials, thus providing an avenue for magnetic materials by design.

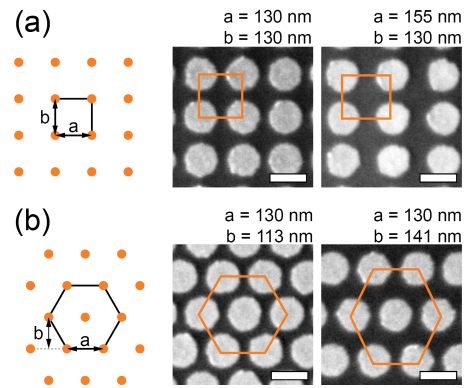


FIG. 1. Scanning electron micrographs of arrays with rectangular (a) and hexagonal (b) lattice symmetry and with lattice constants a and b , as defined in the schematics on the left. The scale bars are 100 nm.

Arrays of ferromagnetic nanodisks with nominal diameter 100 nm and thickness 4.5 nm were patterned on a silicon wafer using electron beam lithography followed by electron beam evaporation of $\text{Ni}_{0.81}\text{Fe}_{0.19}$ (permalloy) and lift-off. A 2 nm thick Al capping layer was deposited on top to prevent oxidation of the permalloy. The disks were arranged on square and hexagonal lattices, respectively, with lattice constants a and b , as shown in Fig. 1. Additional lattices were prepared with an incremental increase in one of the two lattice constants and thus in the separation of the nanomagnet chains. The stretched square and hexagonal lattices then become rectangular and face-centered rectangular, respectively. For simplicity, we refer to the face-centered rectangular lattices as hexagonal. The arrays have overall dimensions of approximately $20\ \mu\text{m} \times 20\ \mu\text{m}$ and are truncated to a square or hexagonal shape. For the hexagon-bound arrays, their termination is chosen to ensure an invariable number of disks along every edge. Scanning electron micrographs of the arrays show that the circular disks are well-defined with an average elliptic distortion of less than 5%.

Magnetic contrast images were recorded using XMCD-PEEM at the SIM beamline of the Swiss Light Source.¹⁶ The sample was rotated in-plane in order to obtain magnetic contrast along two perpendicular directions. Be-

^{a)}Electronic mail: erik.folven@ntnu.no

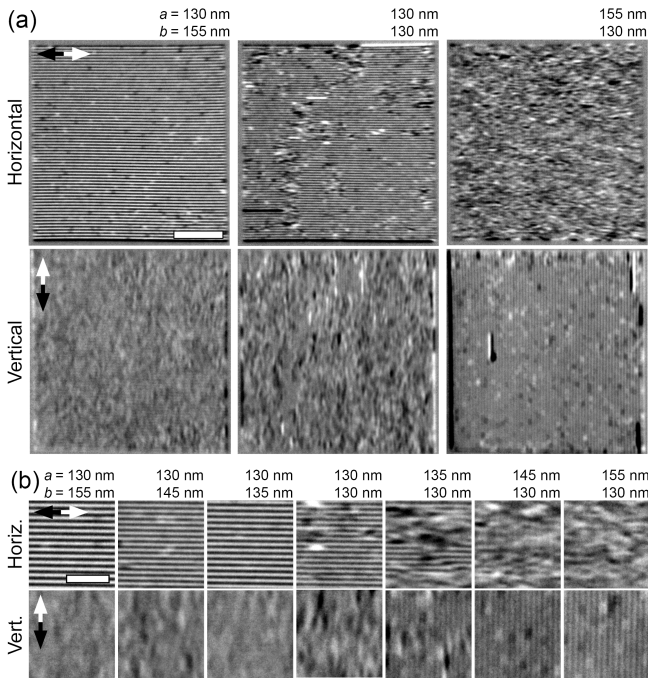


FIG. 2. XMCD-PEEM micrographs of rectangular lattices with $20\ \mu\text{m}$ field of view (a) and $2\ \mu\text{m}$ field of view (b). The XMCD-PEEM contrast is indicated by the black/white double arrow. The scale bars are $10\ \mu\text{m}$ (a) and $1\ \mu\text{m}$ (b).

fore imaging, the arrays were heated to approximately 500 K. At this temperature the magnetic contrast in the arrays vanished, suggesting superparamagnetic behavior of the individual nanomagnets. Subsequent images were recorded at room temperature.

Fig. 2a shows XMCD-PEEM micrographs of three arrays with rectangular lattice symmetry. Magnified views of the center section of seven such arrays are displayed in Fig. 2b. The rectangular lattice with $a = 130\ \text{nm}$ and $b = 155\ \text{nm}$ shows a pattern of black and white horizontal stripes extending throughout the entire array, every stripe corresponding to one chain of nanomagnets. This pattern implies magnetization along horizontal chains with the direction alternating between neighboring chains, i.e., antiferromagnetic order. This is one of two degenerate ground states predicted for an ideal square lattice of point dipoles.¹³

The horizontal stripes predominate for a spacing $b \geq 130\ \text{nm}$ between the chains, cf. Fig. 2b. For the square lattice $a = b = 130\ \text{nm}$, magnetic contrast can be discerned along both the horizontal and the vertical direction. However, horizontal stripes prevail even though the symmetry of the square lattice cannot explain this preference over vertical stripes. This finding could be explained by a small elliptic distortion of the lithographically patterned disks.⁷ Based on scanning electron microscopy image analysis of the square lattice array with $a = b = 130\ \text{nm}$ we find an 4% elliptic distortion of these disks with an average major axis orientation of -38° with

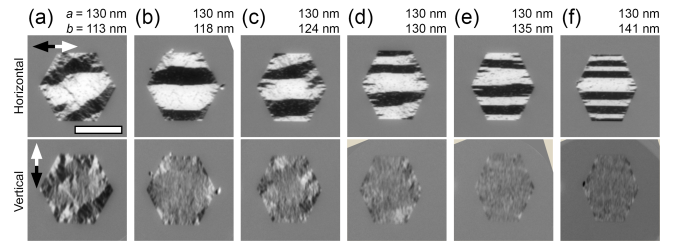


FIG. 3. XMCD-PEEM micrographs of hexagon-bound hexagonal lattices. The XMCD-PEEM contrast is indicated by the black/white double arrow. The lattice parameter b is gradually increased from $113\ \text{nm}$ in (a) to $141\ \text{nm}$ in (f). The scale bar is $10\ \mu\text{m}$.

the horizontal. For $a = 135\ \text{nm}$, horizontal and vertical stripes appear concurrently in different regions of the array, indicating a balance between lattice anisotropy and disk anisotropy at this spacing. At $a = 155\ \text{nm}$, the stripe pattern runs predominantly in the vertical direction in keeping with a minimum dipolar coupling energy for spin alignment along the close-packed direction of the array.

XMCD-PEEM micrographs of the hexagon-bound hexagonal lattices are shown in Fig. 3. These arrays display stripes (with homogeneous contrast) several micrometers wide, which implies ferromagnetic alignment across tens of elements. The length of the domains extends across the arrays.

The undistorted hexagonal lattice (Fig. 3a) exhibits a six-fold symmetry. However, the magnetization observed for this lattice is oriented predominantly along the horizontal direction, similar to that of the undistorted square lattice. With increasing lattice parameter b , i.e., the vertical separation of the nanomagnet chains, the magnetization is aligned distinctly along the horizontal direction. We also note that the number of stripe domains increases with the chain separation.

Corresponding domain patterns for square-bound hexagonal lattices are shown in Fig. 4. In the same way as for hexagon-bound arrays, magnetic stripe domains extend across the entire array. For $a = 130\ \text{nm}$ and $b = 113\ \text{nm}$, the magnetic contrast in the XMCD-PEEM images with the x rays incident along the horizontal (Fig. 4 top) and vertical (Fig. 4 bottom) directions is almost identical, indicating that the domains are magnetized along the diagonal of the square. When the lattice is stretched vertically by increasing b , the dipolar-coupled magnets form horizontal domains, and the number of domains increases.

From our experimental data, we observe that the size of the dipolar ferromagnetic domains changes (Fig. 3a-f). Their width appears to be correlated with the domain length and the lattice parameter b . Kittel¹⁷ has offered a theory for the domain structure in magnetic thin films. For films with stripe domains of alternate out-of-plane magnetization, he finds that the domain width, d , scales with the domain wall energy per unit area, σ_{dw} , the film thickness, T , and the saturation magnetization, M_{sat} as,

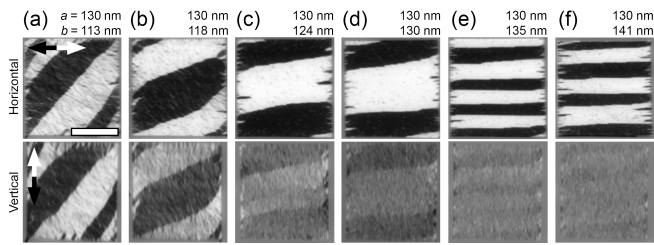


FIG. 4. XMCD-PEEM micrographs of square-bound hexagonal lattices. The XMCD-PEEM contrast is indicated by the black/white double arrow. The lattice parameter b is gradually increased from 113 nm in (a) to 141 nm in (f). The scale bar is 10 μm .

$$d \propto \sqrt{\frac{\sigma_{\text{dw}} T}{M_{\text{sat}}^2}}. \quad (1)$$

The coplanar stripe domains in our hexagonal lattice metamaterial can be explained in terms of this simple scaling law if we replace the film thickness, T , with the domain length, l , which will be the corresponding dimension for in-plane magnetization.

With continuous ferromagnetic thin films, the domain wall energy σ_{dw} is attributed to exchange and anisotropy energies. In a dipolar metamaterial, the exchange energy is absent since the nanomagnets are physically separated. Moreover, the anisotropy contribution to the domain wall energy is zero as long as the magnetization direction changes from one direction to the opposite between two neighboring chains, i.e., the domain wall width is in effect zero. However, as neighboring chains in the hexagonal lattice favor ferromagnetic alignment there must be an energy cost associated with breaking this coupling, which is of dipolar origin. The interchain dipolar coupling falls off exponentially with the chain separation.^{8–10} Hence, as the hexagonal lattice is stretched vertically the domain wall cost for formation of horizontal stripe domains, σ_{dw} , decreases exponentially.

In our data, we observe a reduction of the domain width d as the lattice parameter b is increased (Fig. 3 left to right), in keeping with the decrease in cost of domain wall energy with increasing b .

Eq. 1 predicts a reduced domain width d for shorter domains. This is in good agreement with our observations of a smaller domain width d for the shorter domains close to the top and bottom edges of the hexagon-bound arrays in Fig. 3. The same trend is seen for the square-bound hexagonal lattice when the domains run diagonally across the array (Fig. 4a-d). When the domains are aligned with the horizontal edge of the array, the domain length l is constant. This leads to little variation in domain width d for these arrays (Fig. 4e-f).

We note that the domain width d in Eq. 1 is inversely proportional to the saturation magnetization M_{sat} . In this metamaterial, we take M_{sat} to represent the satu-

ration magnetization of permalloy, $M_{\text{sat}}^{\text{Py}}$, scaled to the nanomagnet areal density, $\pi r^2/ab$, where r is the disk radius and a and b are the respective lattice parameters.

The domain width d is thus related to b in terms of the domain wall energy cost σ_{dw} and saturation magnetization M_{sat} . The observed trend of decreasing domain width with increasing vertical spacing is explained by the predominant exponential reduction of the domain wall energy. In summary, arrays of single-domain ferromagnetic nanodisks were used to form a magnetic metamaterial. In the absence of exchange interactions between the nanomagnets, the dipolar interaction results in long-range magnetic order. The magnetic anisotropy in these lattices was controlled by stretching the arrays in one direction. As a result, the magnetization was found to align with the direction of closest packing. This approach offers a direct way to tailor the magnetic properties of dipolar-coupled metamaterials. We show that the magnetic domain formation can be explained in terms of a modified Kittel’s law. This approach provides a powerful tool for engineering of the domain state in dipolar-coupled magnetic metamaterials.

DATA AVAILABILITY

The data that support the findings of this study are available from the corresponding author upon reasonable request.

ACKNOWLEDGMENTS

We thank T. Tybell for stimulating discussions. Part of this work was performed at the Surface/Interface Microscopy (SIM) beamline of the Swiss Light Source (SLS), Paul Scherrer Institut, Villigen, Switzerland. Partial funding was obtained from the European Union’s Horizon 2020 FET - Open program under grant agreement No. 861618 (SpinENGINE) and the Norwegian PhD Network on Nanotechnology for Microsystems, which is sponsored by the Research Council of Norway, Division of Science, under Contract No. 221860/F60. The Research Council of Norway is acknowledge for support to the Norwegian Micro- and Nanofabrication Facility, NorFab, under Contract No. 245963/F50.

- ¹R. P. Cowburn, D. K. Koltsov, A. O. Adeyeye, M. E. Welland, and D. M. Tricker, “Single-domain circular nanomagnets,” *Physical Review Letters* **83**, 1042–1045 (1999).
- ²S. Bedanta and W. Kleemann, “Supermagnetism,” *Journal of Physics D: Applied Physics* **42**, 013001 (2009).
- ³M. Varón, M. Beleggia, T. Kasama, R. J. Harrison, R. E. Dunin-Borkowski, V. F. Puentes, and C. Frandsen, “Dipolar magnetism in ordered and disordered low-dimensional nanoparticle assemblies,” *Scientific Reports* **3**, 1234 (2013).
- ⁴M. Ewerlin, D. Demirbas, F. Brüßing, O. Petravic, A. A. Ünal, S. Valencia, F. Kronast, and H. Zabel, “Magnetic dipole and higher pole interaction on a square lattice,” *Physical Review Letters* **110**, 177209 (2013).

- ⁵N. Leo, S. Hohenstein, D. Schildknecht, O. Sendetskiy, H. Luetkens, P. M. Derlet, V. Scagnoli, D. Lançon, J. R. L. Mardegan, T. Prokscha, A. Suter, Z. Salman, S. Lee, and L. J. Heyderman, “Collective magnetism in an artificial 2D XY spin system,” *Nature Communications* **9**, 2850 (2018).
- ⁶R. Streubel, N. Kent, S. Dhuey, A. Scholl, S. Kevan, and P. Fischer, “Spatial and temporal correlations of XY macro spins,” *Nano Letters* **18**, 7428–7434 (2018).
- ⁷E. Digernes, S. D. Sløetjes, A. Strømberg, A. D. Bang, F. K. Olsen, E. Arenholz, R. V. Chopdekar, J. K. Grepstad, and E. Folven, “Direct imaging of long-range ferromagnetic and anti-ferromagnetic order in a dipolar metamaterial,” *Physical Review Research* **2**, 013222 (2020).
- ⁸P. Politi, M. G. Pini, and R. Stamps, “Dipolar ground state of planar spins on triangular lattices,” *Physical Review B* **73** (2006).
- ⁹H. Benson and D. L. Mills, “Spin Waves in Thin Films; Dipolar Effects,” *Physical Review* **178**, 839–847 (1969).
- ¹⁰K. De’Bell, A. B. Maclsaac, and J. P. Whitehead, “Dipolar effects in magnetic thin films and quasi-two-dimensional systems,” *Reviews of Modern Physics* **72**, 225–257 (2000).
- ¹¹J. M. Luttinger and L. Tisza, “Theory of dipole interaction in crystals,” *Physical Review* **70**, 954–964 (1946).
- ¹²J. M. Luttinger and L. Tisza, “Errata: Theory of dipole interaction in crystals [Phys. Rev. 70, 954 (1946)],” *Physical Review* **72**, 257–257 (1947).
- ¹³V. M. Rozenbaum, “Vibrational and orientational states of surface atomic groups,” *Soviet Physics Uspekhi* **34**, 883–902 (1991).
- ¹⁴P. Politi and M. G. Pini, “Dipolar interaction between two-dimensional magnetic particles,” *Physical Review B* **66** (2002).
- ¹⁵R. F. Wang, C. Nisoli, R. S. Freitas, J. Li, W. McConville, B. J. Cooley, M. S. Lund, N. Samarth, C. Leighton, V. H. Crespi, and P. Schiffer, “Artificial ‘spin ice’ in a geometrically frustrated lattice of nanoscale ferromagnetic islands,” *Nature* **439**, 303–306 (2006).
- ¹⁶L. Le Guyader, A. Kleibert, A. Fraile Rodríguez, S. El Mousaoui, A. Balan, M. Buzzi, J. Raabe, and F. Nolting, “Studying nanomagnets and magnetic heterostructures with X-ray PEEM at the Swiss Light Source,” *Journal of Electron Spectroscopy and Related Phenomena* **185**, 371–380 (2012).
- ¹⁷C. Kittel, “Theory of the structure of ferromagnetic domains in films and small particles,” *Physical Review* **70**, 965–971 (1946).